

Receiver Clock Reset, Cycle Slip Detection, and Receiver Autonomous Integrity Monitoring

Kai Borre

Aalborg University, Denmark



Galileo Network November 17, 2006



Gross Errors Influencing the Receiver Position

We have more observations (pseudorange) m than unknowns $n = 4$, $m > n$, and we want to estimate the receiver position by using a least-squares procedure.

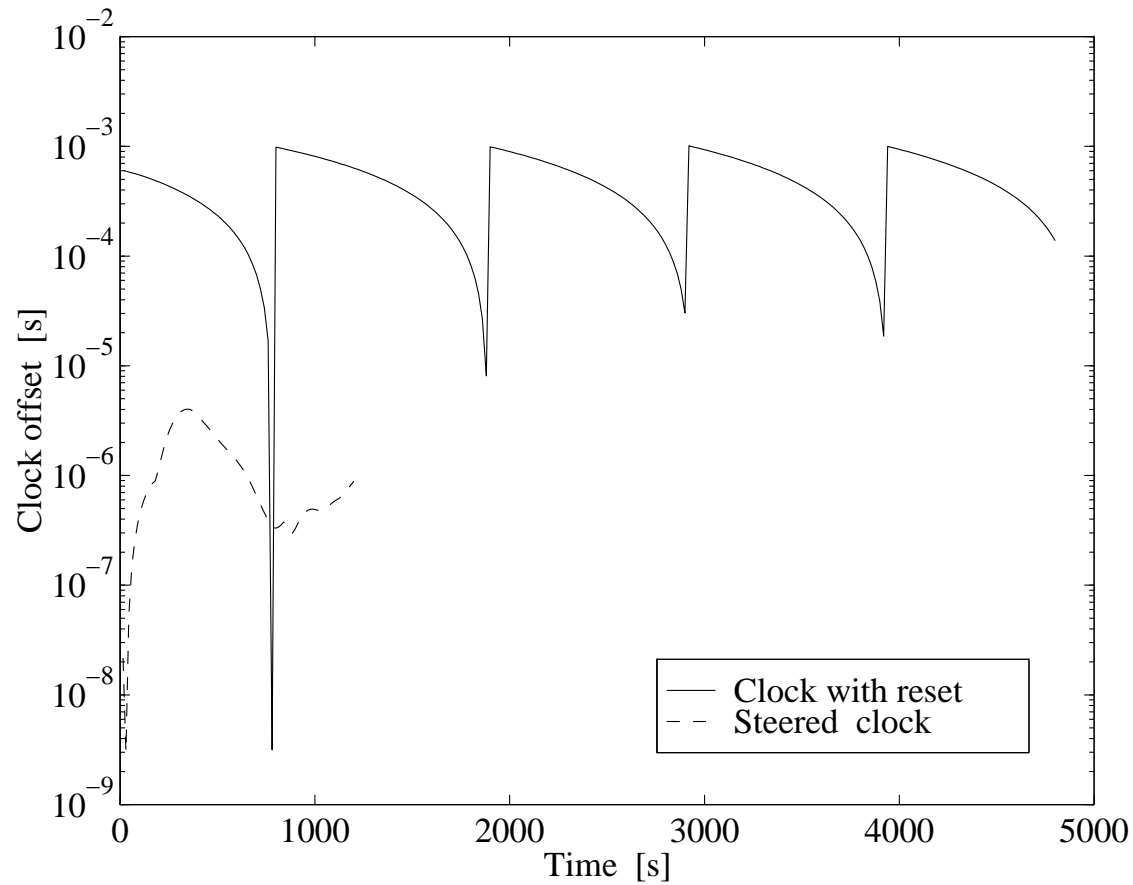
We start by investigating *gross errors*. They may occur in two ways:

1. Receiver clock reset
2. Cycle slips

Next, Receiver Autonomous Integrity Monitoring (RAIM) is expected to detect pseudorange biases that lead to positioning failures.



Receiver Clock Reset



Offsets for different receiver types. The clock reset is 1 millisecond.



Galileo Network November 17, 2006



RINEX

```
2.10          OBSERVATION DATA      G (GPS)          RINEX VERSION / TYPE
JPS2RIN 1.07   RUN BY                  04-SEP-01 13:20   PGM / RUN BY / DATE
build October 30, 2000 (c) Topcon Positioning Systems COMMENT
RUN BY;COMMENT;MARKER NAME;MARKER NUMBER;OBSERVER;AGENCY; COMMENT
ANT #; ANT TYPE - You can set in profile.          COMMENT
kail0001.jps                                       COMMENT
Site                                                MARKER NAME
                                                    MARKER NUMBER
OBSERVER          AGENCY                OBSERVER / AGENCY
MT301513219       JPS EUROCARD           2.2 Apr,25,2001 r REC # / TYPE / VERS
kail0001          -Unknown-              ANT # / TYPE
  3427819.3209    603664.0433   5326880.6438    APPROX POSITION XYZ
           0.0000         0.0000         0.0000    ANTENNA: DELTA H/E/N
    1      1                                     WAVELENGTH FACT L1/2
2001      9      4      9      40      0.0000000    GPS    TIME OF FIRST OBS
2001      9      4      9      40      22.0000000    GPS    TIME OF LAST OBS
    1.000    INTERVAL
    13      LEAP SECONDS
    7      # OF SATELLITES
```



Galileo Network November 17, 2006



	7	C1	P1	P2	L1	L2	# / TYPES OF OBSERV
G 1	23	23	23	23	23	23	PRN / # OF OBS
G 4	23	23	23	23	23	23	PRN / # OF OBS
G 7	23	23	23	23	23	23	PRN / # OF OBS
G13	23	23	23	23	23	23	PRN / # OF OBS
G20	23	23	23	23	23	23	PRN / # OF OBS
G24	23	23	23	23	23	23	PRN / # OF OBS
G25	23	23	23	23	23	23	PRN / # OF OBS
							END OF HEADER

```

01  9  4  9 40  0.0000000  0  7G 1G 4G 7G13G20G24G25
20532012.14648  20532011.55846  20532016.22546  107896448.4014  84075170.1284
21255524.69947  21255524.94445  21255529.02045  111698540.8774  87037834.1244
24648794.02245  24648792.88941  24648801.63741  129530300.6484  100932694.9344
21267718.45748  21267718.52445  21267722.00945  111762613.2534  87087766.9504
21900010.88847  21900009.74444  21900015.95344  115085325.1934  89676892.5064
23828505.41246  23828504.07842  23828511.81542  125219643.5474  97573763.5014
24104647.59546  24104646.97742  24104654.81342  126670763.8784  98704504.1444

```

```

01  9  4  9 40  1.0000000  0  7G 1G 4G 7G13G20G24G25

```

...



Galileo Network November 17, 2006



M-code for Repair of Receiver Clock Offset

```
% Repair of clock reset of 1ms ~ 299 km; affects only pseudoranges
i1 = find(abs(DP(1,:)) > 280000);

for j = i1
    if DP(:,j) < 0
        DP(:,j) = DP(:,j)+299792.458;
    else
        DP(:,j) = DP(:,j)-299792.458;
    end
end
end
```



Galileo Network November 17, 2006



Cycle Slip Detection

Any professional GPS software needs to check for cycle slips; they spoil the carrier phase observations.

The preliminary data validation can be based on the single differenced observations. The goal is to detect cycle slips and outliers in the GPS single difference observations without using any external information with regard to satellite and receiver dynamics, their clock behavior and atmospheric effects. It is done independently for each satellite. There is therefore no minimum number of satellites required for this so-called *integrity monitoring* to work. The following is based on an idea by Kees de Jong (1998).

The dual-frequency single difference measurement model cannot be used directly as it is, since this model is singular. In order to make it regular, a reparametrization has to be performed.



Let $\alpha = (f_1/f_2)^2$, and let hardware delays be denoted η , then the measurement model for epoch k reads

$$\begin{bmatrix} P_1 \\ P_2 \\ \Phi_1 \\ \Phi_2 \end{bmatrix}_k = \begin{bmatrix} 1 \\ 1 \\ 1 \\ 1 \end{bmatrix} [\rho + c dt_i + T + I + \eta_{p1}]_k + \begin{bmatrix} 0 \\ \eta_{P_2} - \eta_{P_1} + (\alpha - 1)I_k \\ \eta_{\Phi_1} - \eta_{P_1} - 2I_k + \lambda_1 N_1 \\ \eta_{\Phi_2} - \eta_{P_1} + (-\alpha - 1)I_k + \lambda_2 N_2 \end{bmatrix} = \begin{bmatrix} 1 \\ 1 \\ 1 \\ 1 \end{bmatrix} R_k + \begin{bmatrix} 0 & 0 & 0 \\ \alpha - 1 & 0 & 0 \\ 0 & -2 & 0 \\ 0 & 0 & -\alpha - 1 \end{bmatrix} \begin{bmatrix} B_1 \\ B_2 \\ B_3 \end{bmatrix}_k \quad (1)$$

with covariance matrix $\Sigma_b = 2\Sigma$ and

$$\Sigma = \begin{bmatrix} \sigma_{P_1}^2 & & & \\ & \sigma_{P_2}^2 & & \\ & & \sigma_{\Phi_1}^2 & \\ & & & \sigma_{\Phi_2}^2 \end{bmatrix}.$$



Parameter R_k in general does not change smoothly with time and is therefore hard to model using e.g. low-degree polynomials. It will therefore be eliminated by pre-multiplying the left and right sides of the above measurement model by the transformation matrix T , defined as

$$T = \begin{bmatrix} -1 & 1 & 0 & 0 \\ -1 & 0 & 1 & 0 \\ -1 & 0 & 0 & 1 \end{bmatrix}$$

resulting in

$$\begin{bmatrix} P_2 - P_1 \\ \Phi_1 - P_1 \\ \Phi_2 - P_1 \end{bmatrix}_k = \begin{bmatrix} \alpha - 1 & 0 & 0 \\ 0 & -2 & 0 \\ 0 & 0 & -\alpha - 1 \end{bmatrix} \begin{bmatrix} B_1 \\ B_2 \\ B_3 \end{bmatrix}_k$$

with covariance matrix $T \Sigma_b T^T$. The parameters B_1 , B_2 , and B_3 are linear combinations of the time-dependent ionospheric effect and the constant hardware delays and carrier ambiguities. The ionospheric effect will be modeled as a first order polynomial, i.e., as a bias I_k and a drift \dot{I}_k . The dynamic model reads

$$\begin{bmatrix} I \\ \dot{I} \end{bmatrix}_k = \begin{bmatrix} 1 & t_k - t_{k-1} \\ 0 & 1 \end{bmatrix} \begin{bmatrix} I \\ \dot{I} \end{bmatrix}_{k-1}$$



The dynamic model for all parameters then becomes

$$\begin{bmatrix} B_1 \\ B_2 \\ B_3 \\ \dot{i} \end{bmatrix}_k = \begin{bmatrix} 1 & 0 & 0 & t_k - t_{k-1} \\ 0 & 1 & 0 & t_k - t_{k-1} \\ 0 & 0 & 1 & t_k - t_{k-1} \\ 0 & 0 & 0 & 1 \end{bmatrix} \begin{bmatrix} B_1 \\ B_2 \\ B_3 \\ \dot{i} \end{bmatrix}_{k-1}$$

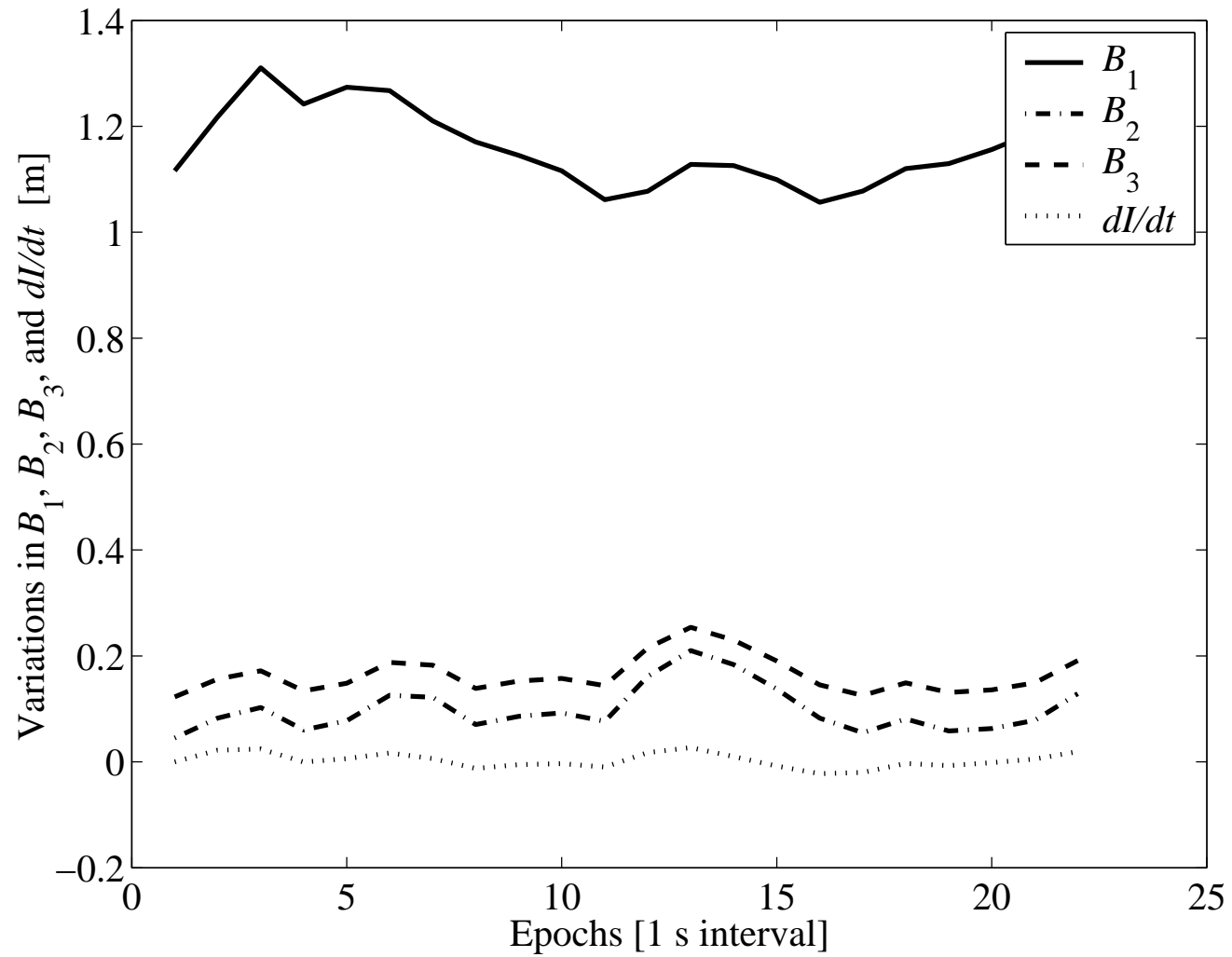
and the measurement model

$$\begin{bmatrix} P_2 - P_1 \\ \Phi_1 - P_1 \\ \Phi_2 - P_1 \end{bmatrix}_k = \begin{bmatrix} \alpha - 1 & 0 & 0 & 0 \\ 0 & -2 & 0 & 0 \\ 0 & 0 & -\alpha - 1 & 0 \end{bmatrix} \begin{bmatrix} B_1 \\ B_2 \\ B_3 \\ \dot{i} \end{bmatrix}_k .$$

With the above measurement and dynamic models it is possible to detect cycle slips as small as one cycle in the carrier observations, without using any external information, even for relatively large observation intervals (or data gaps) $t_k - t_{k-1}$.



Check of Cycle Slips for PRN 1



Galileo Network November 17, 2006



RAIM and FDE

Receiver Autonomous Integrity Monitoring (RAIM) with Fault Detection and Exclusion (FDE) is currently a major technique for GNSS in many safety-critical civil aviation applications. It has been with us since ca. 1990.

Let the $n \times 1$ vector of unknowns be denoted \mathbf{x} , the $m \times 1$ vector of observations be denoted \mathbf{b} , and A is an $m \times n$ matrix and the pertinent linear observation equation is:

$$A\mathbf{x} = \mathbf{b} + \mathbf{e}, \quad \text{and} \quad \Sigma_{\mathbf{b}} = \sigma_b^2 I. \quad (2)$$

The vector \mathbf{e} contains residual errors in the observations.

RAIM is activated for $m \geq 5$. Presently there is no standardized RAIM method.

We shall present the simplest RAIM fault detection based on the residual norm $\|\mathbf{e}\|$.



We define the *position error* as

$$\delta \mathbf{x} = \mathbf{x} - \hat{\mathbf{x}} = \mathbf{x} - (A^T A)^{-1} A^T \mathbf{b} = \mathbf{x} - (A^T A)^{-1} A^T (A \mathbf{x} - \mathbf{e}) = (A^T A)^{-1} A^T \mathbf{e}. \quad (3)$$

The estimated residuals $\hat{\mathbf{e}}$ equals the observations \mathbf{b} minus the estimated observations

$$\hat{\mathbf{e}} = \mathbf{b} - A \hat{\mathbf{x}} = (I - A(A^T A)^{-1} A^T) \mathbf{b} = S \mathbf{b}. \quad (4)$$

The residual vector $\hat{\mathbf{e}}$ is in the left nullspace of A . This means $A^T (\mathbf{b} - A \hat{\mathbf{x}}) = 0$ which is the normal equations.

There are 4 constraints among the m components of $\hat{\mathbf{e}}$, namely three for the coordinates (x, y, z) and one for the receiver clock offset dt .



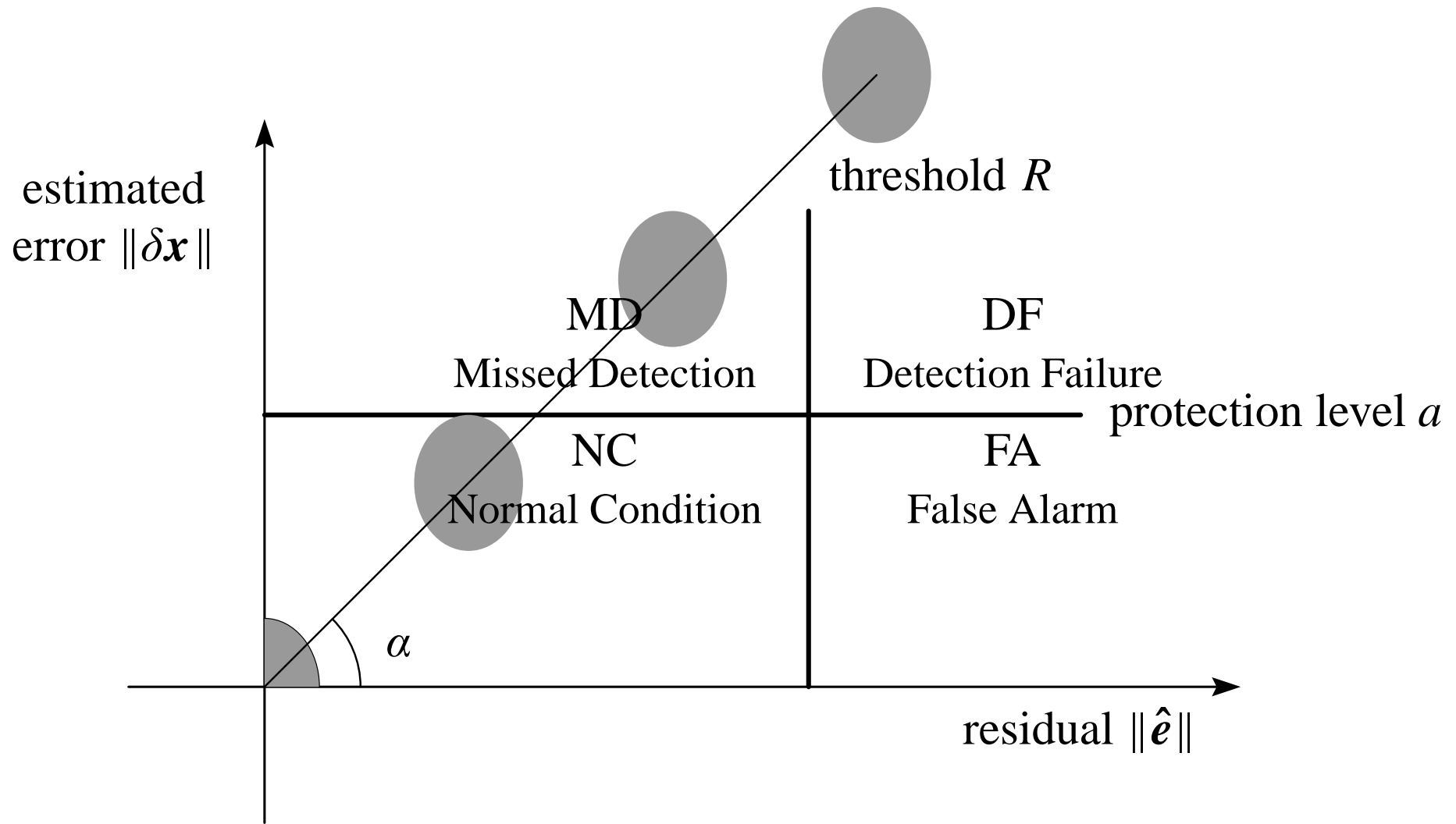


Figure 1: Basic RAIM state
Galileo Network November 17, 2006



In the event that the position error exceeds a predefined protection radius a , but $\|\hat{\mathbf{e}}\| < R$, a missed detection has occurred, case II; the corresponding probability is defined as

$$P(\text{MD}) = P(\|\hat{\mathbf{e}}\| < R, \|\delta\mathbf{x}\| > a). \quad (5)$$

In general a condition between $\|\hat{\mathbf{e}}\|$ and $\|\delta\mathbf{x}\|$ will exist. The degree of this correlation must be quantified to demonstrate the integrity monitoring capability of RAIM-based fault detection.

The residual $\hat{\mathbf{e}}$ and the position error $\delta\mathbf{x}$ will scale proportionally. Hence the NC confidence ellipse will slide up the *failure mode axis* with slope α .

The components of $\hat{\mathbf{e}}$ are dependent as they are computed from (4):

$$\hat{\mathbf{e}} = S\mathbf{b}.$$



The corresponding covariance matrix is

$$\Sigma_{\hat{e}} = S \Sigma_b S^T = \sigma_b^2 S S^T = \sigma_b^2 S. \quad (6)$$

Note that Σ_b is diagonal, while $\Sigma_{\hat{e}}$ is a full matrix!

In order to identify the probability distribution of the residuals we need to transform the vector \hat{e} into independent components. This is done by an old trick which implies multiplication to the left with $\frac{1}{\sigma_b} W$. This factor comes from the Cholesky decomposition of the covariance matrix

$$\Sigma_{\hat{e}} = (\sigma_b W^{-1})(\sigma_b W^{-T}).$$

The transformed residual vector

$$\hat{e}^* = \frac{1}{\sigma_b} W \hat{e}$$



will have independent components.

Under normal conditions (NC) (small $\|\hat{\mathbf{e}}\|$) the weighted sum of squares is

$$\hat{\mathbf{e}}^T \frac{1}{\sigma_b^2} \mathbf{W}^T \mathbf{W} \hat{\mathbf{e}} = \hat{\mathbf{e}}^{*T} \hat{\mathbf{e}}^*. \quad (7)$$

The vector $\hat{\mathbf{e}}^*$ is gaussian and independent and identically distributed with zero mean and variance 1:

$$\|\hat{\mathbf{e}}^*\| \sim \chi_{m-n}^2, \quad m > n. \quad (8)$$

A residual threshold can be set analytically using (8) to achieve any desired probability of false alarm (FA) under normal error conditions (NC):



$$P(\text{FA} \mid \text{NC}) = P(\|\hat{\mathbf{e}}^*\| > R \mid \text{NC})$$

$$= \frac{1}{2^{(m-n)/2} \Gamma\left(\frac{m-n}{2}\right)} \int_{R^2/\sigma_b^2}^{\infty} s^{\left(\frac{m-n}{2}-1\right)} e^{-s/2} ds. \quad (9)$$

Given the values of $m - n$ and $P(\text{FA} \mid \text{NC})$ we may solve (9) for R . The result is plotted in Figure 2.



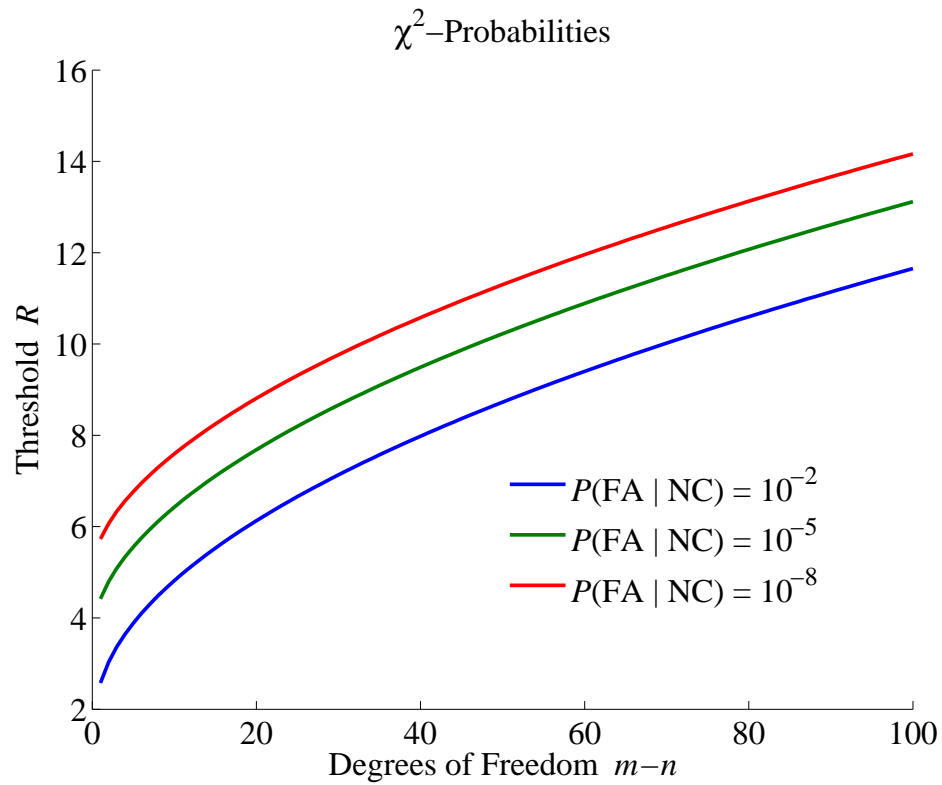


Figure 2: Probability of false alarm



The *M*-code for plotting Figure 2 is as follows:

```
false_alarm = [0.01, 0.00001, 0.00000001];
sigma_b = 1;
for i = 1:length(false_alarm)
    R(:,i) = sigma_b^2 * sqrt(chi2inv(1 - false_alarm(i), 1:100));
end
h1 = plot(R)
set(h1, 'linewidth', 1)
xlabel('Degrees of Freedom {\it m - n}', 'fontsize', 18)
ylabel('Threshold {\it R}', 'fontsize', 18)
title('{\it \chi}^2 - Probabilities', 'fontsize', 18)
legend('{\it P}(FA | NC) = 10^{-2}', ...
    '{\it P}(FA | NC) = 10^{-5}', '{\it P}(FA | NC) = 10^{-8}')
set(gca, 'fontsize', 18)
box off
pause % opportunity to move legend
legend('boxoff')
print -depsc2 raim6
```



In equation (3) the position error

$$\delta \mathbf{x} = (A^T A)^{-1} A^T \mathbf{e}$$

is defined in a 3-D Cartesian coordinate system. However, for practical use a local topocentric coordinate system $\delta \mathbf{x}_{ENU} = (e, n, u)$ is more appropriate. The transformation matrix F is given as

$$F = \begin{bmatrix} -\sin \lambda & \cos \lambda & 0 \\ -\sin \phi \cos \lambda & -\sin \phi \sin \lambda & \cos \phi \\ \cos \phi \cos \lambda & \cos \phi \sin \lambda & \sin \phi \end{bmatrix}. \quad (10)$$

In the following we only consider the three coordinates (X, Y, Z) . So we delete the last column of A and get a new matrix $A_0 = A(:, 1 : 3)$. Similarly we delete the last element of $\delta \mathbf{x}$ and define $\delta \mathbf{x}_0 = \delta \mathbf{x}(1 : 3)$.



Hence

$$\delta \mathbf{x}_{ENU} = \begin{bmatrix} e \\ n \\ u \end{bmatrix} = F \delta \mathbf{x}_0 = F (A_0^T A_0)^{-1} A_0^T \mathbf{e} = M \mathbf{e}. \quad (11)$$

Note that rows 1 and 2 of the $3 \times m$ matrix M relate to x and y . Note also that multiplication by F changes the coordinate basis from the geocentric to the topocentric system!

Imagine now a failure of magnitude β in satellite i :

$$\mathbf{e} = [0 \ \dots \ 0 \ \beta \ 0 \ \dots \ 0]^T. \quad (12)$$

We compute the norm squared for this special choice of \mathbf{e} :

$$\|\delta \mathbf{x}_{ENU}\|^2 = \mathbf{e}^T M^T M \mathbf{e}.$$



Because the many zeros in \mathbf{e} this simplifies to

$$\|\delta\mathbf{x}_{ENU}\|^2 = (m_{1i}^2 + m_{2i}^2)\beta^2.$$

From (4) we have $\hat{\mathbf{e}} = S\mathbf{b}$ or

$$\|\hat{\mathbf{e}}\|^2 = \hat{\mathbf{e}}^T \hat{\mathbf{e}} = \mathbf{b}^T S^T S \mathbf{b} = s_{ii} \beta^2$$

as $S^T S = S$. The diagonal entry (i, i) of S is called s_{ii} . Now

$$\|\delta\mathbf{x}_{ENU}\|^2 = \frac{m_{1i}^2 + m_{2i}^2}{s_{ii}} \|\hat{\mathbf{e}}\|^2$$

or

$$\|\delta\mathbf{x}_{ENU}\| = \sqrt{\frac{m_{1i}^2 + m_{2i}^2}{s_{ii}}} \|\hat{\mathbf{e}}\|. \quad (13)$$



This is the equation for a straight line through the origin and with slope α_i . We compute the slope α_i of the failure mode axis related to satellite i as

$$\alpha_i = \sqrt{\frac{m_{1i}^2 + m_{2i}^2}{s_{ii}}}. \quad (14)$$

The slope values are computed for all $i = 1, \dots, m$ and the corresponding lines are depicted in Figure 3.

The slope α_i provides a measure of the difficulty in accurately detecting a fault in presence of noise: The larger the slope, the more difficult it is to detect the fault.



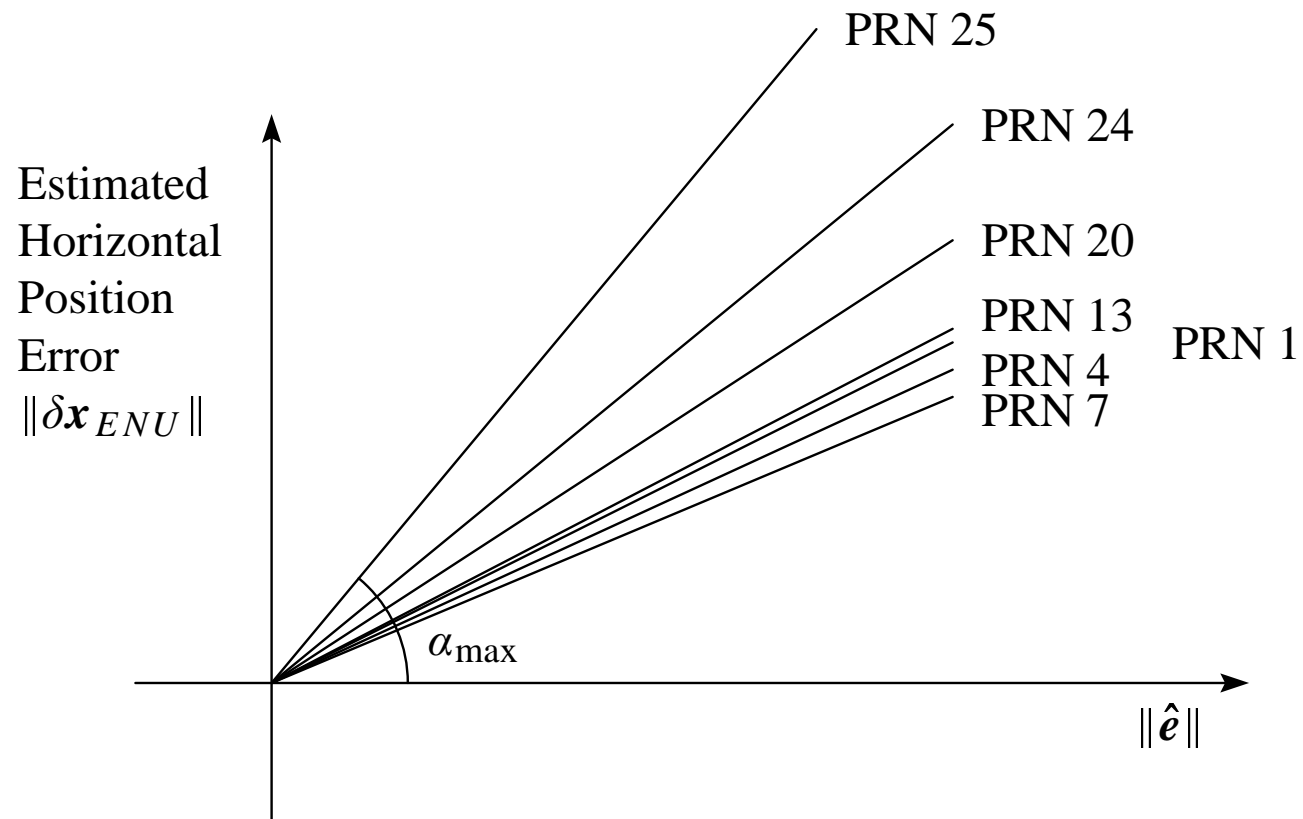


Figure 3: Characteristic slopes for seven visible satellites



The failure mode axes in Figure 3 through the origin with slope α_i are determined exclusively from the geometry determined by the satellites and the receiver. The mode axis with maximum value of α_i is called α_{\max} and the *horizontal protection level* (HPL) is defined as

$$\text{HPL} = \alpha_{\max} \sigma_0 \quad (15)$$

where σ_0 is the standard deviation of the pseudoranges $\sigma_0 = \sqrt{\frac{\hat{\mathbf{e}}^T \Sigma_b^{-1} \hat{\mathbf{e}}}{n-4}}$.

In Figure 1 a horizontal line constraint is drawn to represent the protection radius a . Note that it is possible for small failure magnitudes, that accuracy specification not be breached. Also shown in this figure is the residual threshold R .

The resulting RAIM fault detection algorithm is a simple one: Check the residual statistic to see if it is larger than the threshold R . If so, a system failure is declared. Given this simple algorithm, four outcomes are possible.



Under *normal operation*, the position error $\|\delta\mathbf{x}\|$ does not exceed the protection radius a and the residual is smaller than the threshold R , case III. If the position error does not exceed the protection radius a , but the residual is larger than the threshold R , a *false alarm* has occurred, case IV. When both protection radius and residual threshold have been breached, a *detection failure* has occurred, case I. Finally, a *missed detection* happens when the position error $\|\delta\mathbf{x}\|$ is larger than the protection radius a , but the residual is smaller than the threshold R , case II. In the general case, of course, more than one failure mode exists. However, this presentation does not deal with that case.

It is important to note explicitly that integrity risk can always be reduced at the expense of accuracy, continuity, and availability.

Hwang et al. (2005) investigates RAIM in case of non-uniform weighted observations and multiple faults.



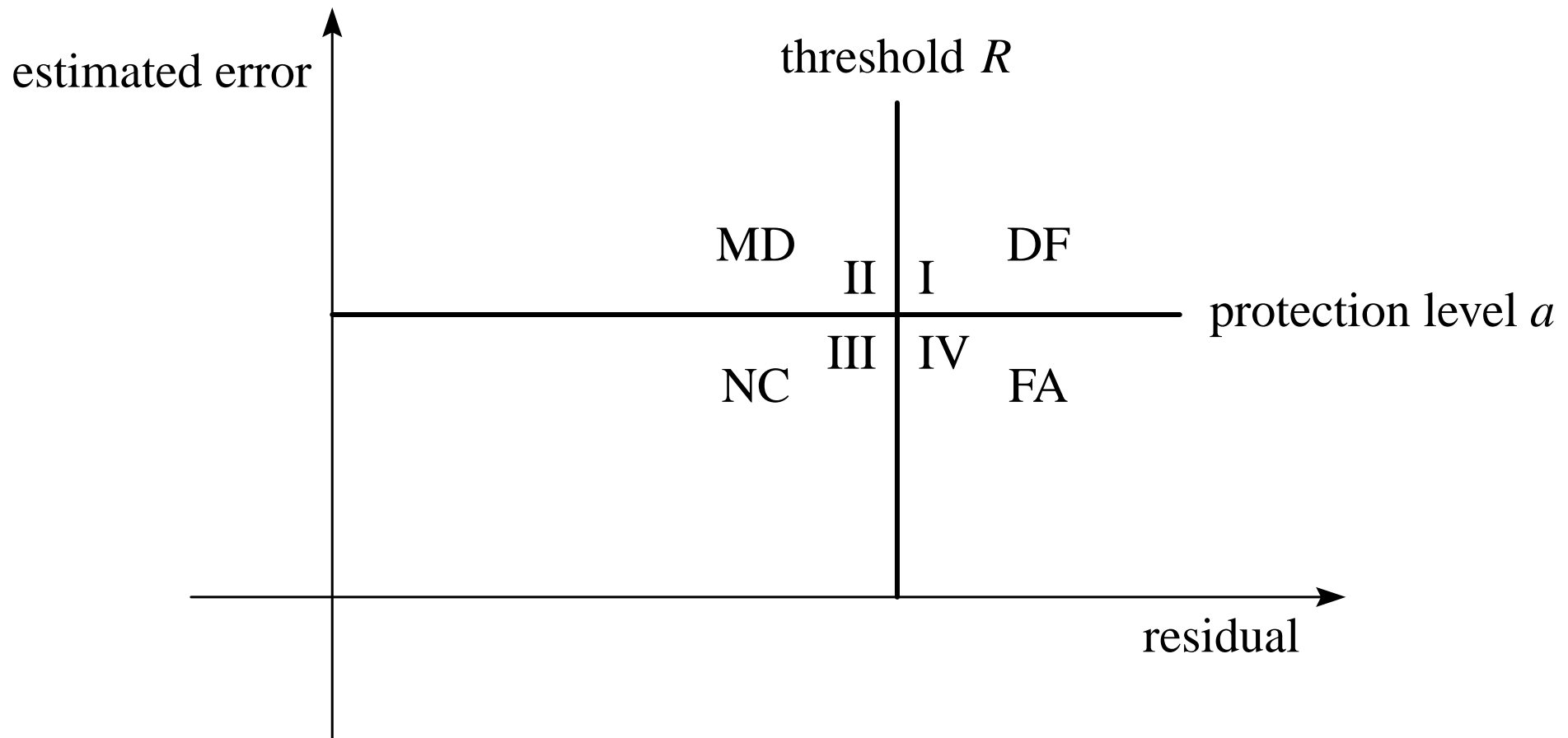


Figure 4: RAIM status, repeated



If the HPL is below the alert limit, RAIM is said to be available for that epoch. Since HPL is dependent on satellite geometry, it must be computed for each epoch and each position.

Numerical Values

RTCA, SC159 defines the maximum allowable probabilities for a false alert as $P(\text{FA}) = 2 \times 10^{-5}$ and a missed detection as $P(\text{MD}) = 10^{-3}$.

The standard deviation σ_b of a pseudorange can be set equal to 3.8 m.

The protection level a (also called horizontal alarm limit, HAL) varies according to the application. It could be 12 m, say.



Input to RAIM: The variance σ_b^2 of a pseudorange observation, the coefficient matrix A of the linearized least-squares observation equations, and the maximum allowable probabilities for a false alarm $P(\text{FA})$ and a missed detection $P(\text{MD})$.

Output of the algorithm: Horizontal protection level (HPL) which is the radius of a circle, centered at the true aircraft position that is assured to contain the indicated horizontal position with the given probability of false alert and missed detection.

Similarly for Vertical protection level (VHL)



References

Borre, Kai (2003) The GPS Easy Suite—Matlab code for the GPS newcomer. *GPS Solutions*, **7**: 47–51

de Jong, Kees (1998) Real-time integrity monitoring, ambiguity resolution and kinematic positioning with GPS. In: Proc 2nd European Symp GNSS'98, Toulouse, pp VIII07/1-VIII07/7

Hwang, Patrick Y. & R. Grover Brown (2005) *NIORAIM Integrity Monitoring Performance in Simultaneous Two-Fault Satellite Scenarios*. ION GNSS 18th International Technical Meeting of the Satellite Division, 13–16 September 2005, Long Beach, CA, 1760–1771

Kaplan, Elliott D. & Christopher J. Hegarty (editors) (2006) *Understanding GPS, Principles and Applications*, Second Edition, Artech House, Boston



Galileo Network November 17, 2006



Nikiforov, Igor & Benoît Roturier (2005) *Advanced RAIM Algorithms: First Results*. ION GNSS 18th International Technical Meeting of the Satellite Division, 13–16 September 2005, Long Beach, CA

Pervan, Boris Steven (1996) *Navigation Integrity for Aircraft Precision Landing Using the Global Positioning System*. Dissertation, Stanford University, xvi + 172 pages

Strang, Gilbert & Kai Borre (1997) *Linear Algebra, Geodesy, and GPS*. Wellesley-Cambridge Press, MA. See www.wellesleycambridge.com

